Arabian Journal of Chemistry (2023) **16**, 104914

King Saud University

Arabian Journal of Chemistry

www.ksu.edu.sa
www.sciencedirect.com

ORIGINAL ARTICLE

Preparation of cobalt-ruthenium nanocatalysts supported on nitrogen-doped graphene aerogel and carbon nanotubes in Fischer-Tropsch synthesis

Mohammadreza rezaei Kafrani [a], **Ali Aghababai Beni** [b,*], **Zahra Pournuroz Nodeh** [c]

[a] *Department of Chemical and Petroleum Engineering, Sharif University of Technology, Tehran, Iran*
[b] *Department of Chemical Engineering, Shahrekord Branch, Islamic Azad University, Shahrekord, Iran*
[c] *Department of Chemistry, Lahijan Branch, Islamic Azad University, Lahijan, Iran*

Received 23 January 2023; accepted 10 April 2023
Available online 18 April 2023

KEYWORDS

Cobalt-ruthenium nanocatalysts;
Nitrogen-doped graphene aerogel;
Carbon nanotube;
Fischer-Tropsch;
CO conversion

Abstract In this study, cobalt-ruthenium nanocatalysts supported on nitrogen-doped graphene aerogel (NGA) and carbon nanotubes (CNT) were synthesized using the wet impregnation method for Fischer-Tropsch process with a cobalt to ruthenium ratio of 1:50. The synthesized catalysts underwent various characterizations such as FTIR, ICP, BET, XRD, EDX, TPR and TEM. The performance of the synthesized catalysts was compared to that of a cobalt-ruthenium nanostructured catalyst supported on NGA and CNTs. The catalysts were evaluated in a fixed-bed reactor at 25 bar, with a gas ratio H_2/CO: 2 and Gas Hourly Space Velocity (GHSV) 10,000 ml g^{-1} h^{-1}, at temperatures of 260 °C and 280 °C. The use of NGA as a cobalt catalyst support led to a 70.5% conversion of carbon monoxide and higher methane selectivity. Conversely, the use of CNTs led to 63.7% conversion of carbon monoxide and higher selectivity towards C_{5+} production.

© 2023 The Author(s). Published by Elsevier B.V. on behalf of King Saud University. This is an open access article under the CC BY-NC-ND license (http://creativecommons.org/licenses/by-nc-nd/4.0/).

1. Introduction

The conversion of natural gas to liquid is achieved through a catalytic process known as Fischer-Tropsch synthesis (Piazzi et al., 2022). This process involves converting natural gas, which primarily consists of methane, into liquid hydrocarbons such as gasoline, diesel, and jet fuel (Wang and Astruc, 2018). The purpose of this process is to make natural gas more transportable and usable in a wider range of applications. The catalyst used in this process is typically cobalt, iron or ruthenium supported on an alumina, silica or zeolite catalyst (Sapountzi et al., 2017). The catalyst promotes the reaction between carbon monoxide and hydrogen, which ultimately leads to the formation of liquid hydrocarbons (Taghavi et al., 2017). The choice of support material in catalysts is critical to their effectiveness and durability (Abbas et al., 2020). Recent advancements in nanotechnology have led to the creation of support materials such as metal oxides, carbon-based materials, and zeolites, which have high surface areas and controllable porosity (Hodala et al., 2021). This enables optimization of catalytic activity and selectivity, making them suitable for use in the catalytic conversion of natural gas into liquid (Santos and Alencar, 2020). Additionally, the use of nanoscale support materials allows for recycling of

* Corresponding author at. Tel.: +98-9139781836.
E-mail address: aliaghababai@yahoo.com (A. Aghababai Beni).
Peer review under responsibility of King Saud University.

ELSEVIER Production and hosting by Elsevier

https://doi.org/10.1016/j.arabjc.2023.104914
1878-5352 © 2023 The Author(s). Published by Elsevier B.V. on behalf of King Saud University.
This is an open access article under the CC BY-NC-ND license (http://creativecommons.org/licenses/by-nc-nd/4.0/).

metal contaminants through leaching, a sustainable approach that promotes the reuse of materials in the production of new catalysts (Julkapli and Bagheri, 2015).

Graphene is a two-dimensional material composed of a single layer of carbon atoms arranged in a hexagonal lattice. It has several unique properties, including high surface area, high thermal and electrical conductivity, excellent mechanical strength, and chemical stability. These characteristics have made graphene an attractive material for various applications, including catalysis (Detsios et al., 2022). In the process of converting natural gas into liquid, graphene has been used as a base material in the manufacture of catalysts due to its high surface area and excellent catalytic activity. Graphene-based catalysts have shown great potential in improving the efficiency and selectivity of the Fischer-Tropsch synthesis, where natural gas is converted into liquid hydrocarbons. One example of the use of graphene in the form of nanosheets in the manufacture of catalysts for the conversion of natural gas into liquid is the development of graphene-supported cobalt nanoparticles (Liu et al., 2020). In this process, graphene oxide is reduced to form graphene nanosheets, which are then used as a support material for cobalt nanoparticles. The resulting graphene-supported cobalt nanoparticles have been shown to have excellent catalytic activity and stability, leading to higher yields of liquid hydrocarbons in the Fischer-Tropsch synthesis. Another example is the use of graphene oxide as a support material for iron nanoparticles in the Fischer-Tropsch synthesis (Okoye-Chine et al., 2019). The graphene oxide nanosheets are functionalized with amine groups, which act as anchor sites for the iron nanoparticles. This functionalization process increases the dispersion of the iron nanoparticles on the graphene oxide nanosheets, resulting in higher catalytic activity and selectivity (Li et al., 2016).

The objective of this study is to explore the potential of cobalt and cobalt-ruthenium catalysts, supported on graphene and carbon nanotubes, for the Fischer-Tropsch process. The incipient wetness impregnation method is utilized to synthesize the catalysts with different weight ratios. The physicochemical properties of the catalysts are analyzed using various techniques. Furthermore, the performance of the catalysts is evaluated based on the conversion rate of carbon monoxide and the selectivity of light and heavy products. The results obtained from the study are expected to provide insight into the development of more efficient and selective catalysts for the Fischer-Tropsch process.

2. Experimental

2.1. Materials

The high-purity precursors and promoters utilized for the preparation of cobalt and cobalt-ruthenium catalysts were cobalt nitrate and ruthenium (III) nitrosyl nitrate, respectively, sourced from Sigma-Aldrich. The purity level of these compounds was greater than 99.9%. To fabricate the catalyst supports, nitrogen-doped graphene aerogel (NGA) and multi-walled carbon nanotubes (CNTs) were obtained from Changzhou Sixth Element Materials Technology Co., Ltd.

2.2. Catalyst preparation

To pretreat the graphene, 10 g of the as-received material was mixed with nitric acid solution (40% HNO_3) in a round-bottom flask and refluxed at 120 °C for 8 h. After cooling to room temperature, the sample was filtered and washed multiple times with deionized water until reaching a neutral pH level. The resulting pretreated nitrogen-doped graphene aerogel base material was then dried at 120 °C for 24 h. For the preparation of the graphene-supported cobalt-ruthenium catalysts, predetermined amounts of ruthenium and cobalt with ratios of 1:50, respectively, were dissolved in deionized water. The cobalt-ruthenium mixture was then impregnated onto the nitrogen-doped graphene aerogel using the incipient wetness method. The catalyst sample was left to settle for 24 h before being dried at 120 °C for another 24 h. The sample was then calcined under a nitrogen atmosphere at 380 °C for 6 h. The catalysts synthesized using the pretreated nitrogen-doped graphene aerogel with different nitric acid concentrations were designated as Co-Ru/NGA. The same procedure was carried out for the carbon nanotubes base.

2.3. Characterization

The catalysts were subjected to various characterization techniques to determine their properties. Fourier transform infrared spectroscopy (FTIR) was used to identify functional groups and was performed using a PerkinElmer spectrometer. Powder X-ray diffraction (XRD) was carried out on an X'Pert Pro X-ray diffractometer (PANalytical, the Netherlands) with Cu Kα irradiation (λ = 1.5406 Å) at 40 kV and 30 mA. The morphology of cobalt catalysts on the surface of supports was examined by transmission electron microscopy (TEM) using a Zeiss EM10C (kV 100) device. The Co and Ru loadings of the synthesized catalysts were determined by The Inductively Coupled Plasma Atomic Emission Spectroscopy (ICP-AES) method. The energy-dispersive X-ray spectroscopy (EDX) (JEOL, JED-2300) was used to determine the catalyst compositions. Nitrogen adsorption isotherms were obtained at 77 K using the Brunauer-Emmett-Teller (BET) model to illustrate the N2 adsorption–desorption isotherms of several catalysts. The catalysts underwent H_2-TPR profiling to examine the reducibility of the metal species. The samples (=0.05 g) were purged with helium at 140 °C to eliminate any remaining gases and cooled to 40 °C. Subsequently, 5% H2 in Ar gas was used for TPR analysis, with a flow rate of 40 mL min^{-1} at atmospheric pressure, using the Micrometrics TPD-TPR 2900 analyzer, equipped with a thermal conductivity detector (TCD). The samples were heated linearly at a rate of 10 °Cmin^{-1} up to 850 °C. Using the Micromeritics TPD-TPR 290 system, the quantity of chemisorbed hydrogen on the catalysts was assessed. Initially, a 0.25 g sample was reduced with hydrogen flow at 400 °C for 12 h, followed by cooling to 100 °C while under hydrogen flow. Next, the hydrogen flow was replaced with argon at the same temperature for approximately 30 min, eliminating weakly adsorbed hydrogen. The temperature-programmed desorption (TPD) was then performed by raising the temperature of the samples to 400 °C under argon flow at a ramp rate of 10 °C min^{-1}. The TPD profile obtained was used to determine the dispersion of cobalt and its average crystallite size on the surface. After H2-TPD, 10% oxygen in helium pulses were used to reoxidize the sample at 400 °C to assess the degree of reduction.

2.4. Hydrocarbon synthesis in the reaction system

A tubular down flow, fixed-bed reactor system was employed for Fischer-Tropsch synthesis (Fig. 1). The reactor, consisting of a stainless-steel tube with an inside diameter of 22 mm and a length of 450 mm, was used with 1 g of catalyst. H_2 and CO were added to the reactor at the desired rate using Brooks

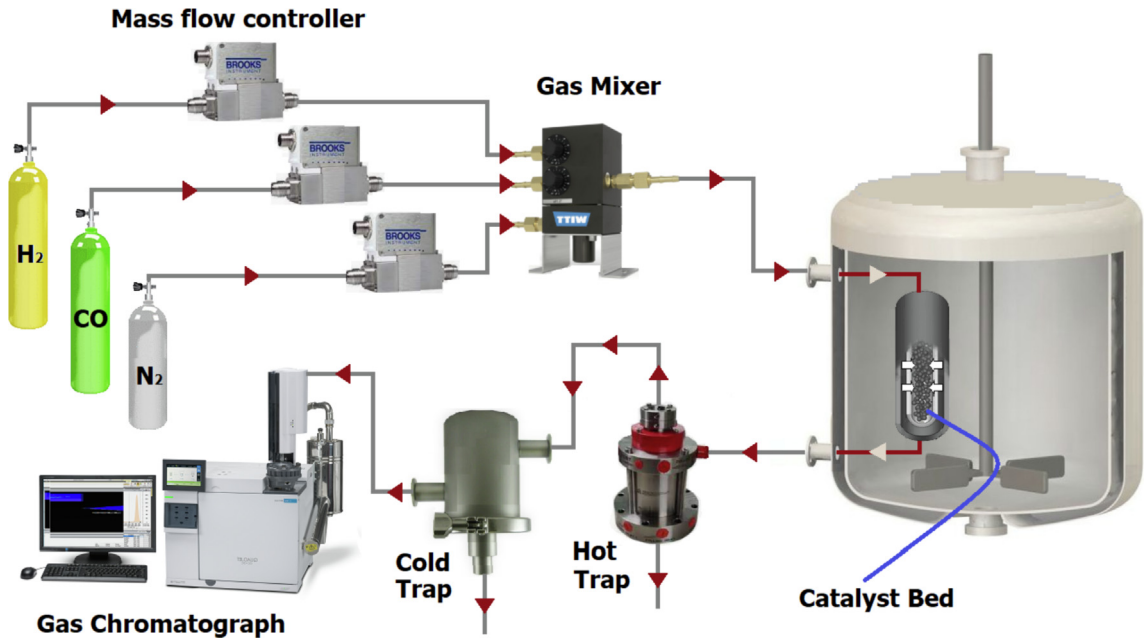

Fig. 1 Experimental set-up.

5850 mass flow controllers. The catalyst was reduced with hydrogen flowing at 400 °C for 12 h. After reduction, a mixture of CO and H_2 was introduced to the reactor at a pressure of 2 MPa, a flow rate of 50 mL min^{-1}, a temperature of 220 °C, and a H_2/CO ratio of 2. Products were removed from the reactor continuously and passed through a hot trap maintained at 120 °C and a cold trap at 0 °C. Gas products were analyzed with time intervals of 2 h for CO, CO_2, and other gaseous products. Liquid products were collected and analyzed using three gas chromatographs. A Shimadzu 4C gas chromatograph was equipped with two connected packed columns, Porapak Q and Molecular Sieve 5 Å, and a thermal conductivity detector (TCD) with argon as a carrier gas for hydrogen analysis. A Varian CP 3800 with a Petrocol Tm DH100 fused silica capillary column and a flame ionization detector (FID) were used for liquid products to provide a complete product distribution. A Varian CP 3800 with a chromosorb column and a thermal conductivity detector (TCD) were used for CO, CO_2, CH_4, and other non-condensable gases. The reactor was placed in a molten salt bath with a stirrer to ensure uniform temperature along the catalytic bed. The bath temperature was controlled by a PID temperature controller.

3. Results and discussion

3.1. FTIR spectra

In Fig. 2**a**, bands were observed at 1089 cm^{-1} corresponding to the oscillation of the carboxyl group bond, and at 1453 cm^{-1} region of the spectrum, indicating the aromatic ring bond. The symmetric and asymmetric C—H stretches were observed for CH_2 and CH_3 at 2898 cm^{-1} and C—H at 582 cm^{-1}. Furthermore, the peaks observed at 1682 cm^{-1} and 3420 cm^{-1} were related to the tensile vibrations of the carbonyl and hydroxyl groups in carboxylic acid, respectively (Vasseghian et al., 2022). These results indicate that the nitric acid treat-

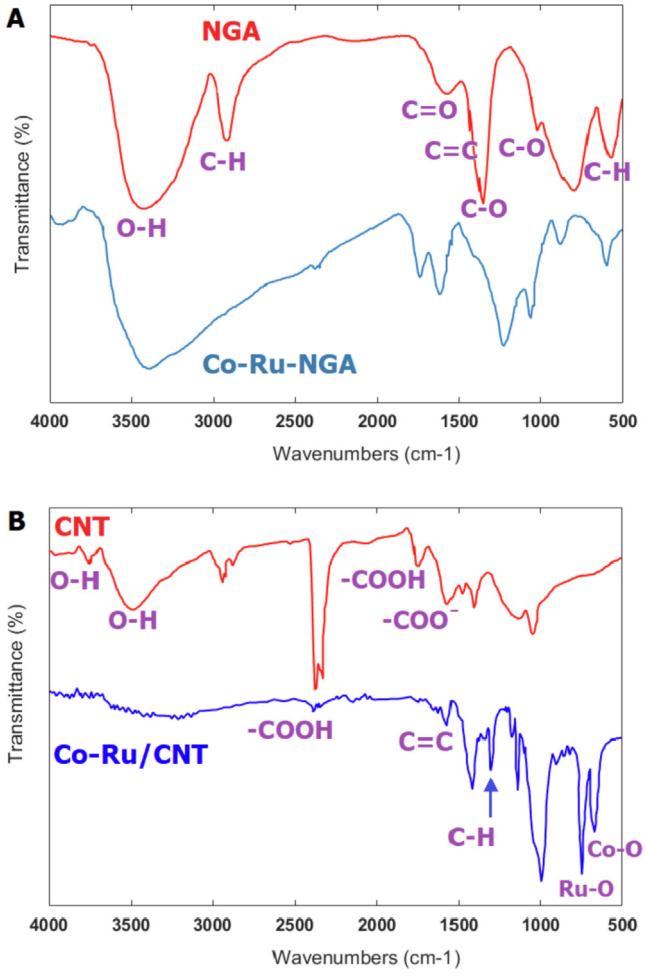

Fig. 2 The FTIR spectrum of NGA, Co-Ru/NGA (a) and CNT, Co-Ru/CNT (b).

ment of nitrogen-doped graphene aerogel led to the formation of carboxyl groups on the surface of nitrogen-doped graphene aerogel. The peak observed at wavelength 1543 cm^{-1} is related to the double bonds in the nitrogen-doped graphene aerogel structure. The FTIR spectrum of ruthenium showed peaks at 516 cm^{-1} and 600 cm^{-1}, which correspond to the Ru—O bond. The FTIR spectrum of cobalt showed peak at 580 cm^{-1}, which correspond to the Co—O bond. The added peaks and shifts of some peaks are attributed to the presence of Co—Ru in the catalyst.

According to Fig. 2**b**, the FTIR of CNTs exhibit four major peaks, indicating the presence of various functional groups. The broad peak at 3425 cm^{-1} is characteristic of the O – H stretch of the hydroxyl group and can be attributed to the oscillation of carboxyl groups. The peak located at 1736 cm^{-1} is associated with the stretch mode of carboxylic groups. The peak at 3728 cm^{-1} is assigned to free hydroxyl groups, while the peak at 2361 cm^{-1} is associated with the O—H stretch from strongly hydrogen-bonded —COOH. Finally, the peak at 1560 cm^{-1} is related to the carboxylate anion stretch mode. Also, FTIR analysis of cobalt and ruthenium coated on CNTs, peaks at 525 cm^{-1} and 601 cm^{-1} were observed, which are related to stretching vibrations of Co—O bond and Ru—O bond. Attributed, respectively. The observed peak at 1630 cm^{-1} was assigned to stretching vibrations of C=C bonds in carbon nanotubes, while the peak at 1380 cm^{-1} was due to bending vibrations of C—H bonds in the same structure.

3.2. ICP analysis

ICP stands for Inductively Coupled Plasma, which is a technique used to determine the elemental composition of a sample. Table 1 presents the results of the ICP analysis, which shows the metal contents of the catalysts. The metal contents were found to be fairly similar and close to the target metal contents of 15 and 1 wt%, which indicates that the synthesis process was successful and the catalysts were prepared as intended. It is important to note that the accuracy and precision of the ICP analysis can be affected by various factors, such as sample preparation, instrument calibration, and matrix effects, among others (Cheng et al., 2021; Wang and Astruc, 2018). (See Table 2.)

3.3. BET test

According to Fig. 3, the BET surface area of the Co-Ru/NGA and Co-Ru/CNT catalysts were comparable, with values of 212 and 199 $m^2\,g^{-1}$, respectively. The pore size distribution, specific volume, and average pore diameter showed a similar

Table 2 The size of Co_3O_4 crystals diameter in structure of the catalyst based on the calculation with Scherer's equation.

Catalyst	Co_3O_4 diameter (nm)	Reference
Co-Ru/NGA	12.49	In this work
Co-Ru/CNT	13.74	In this work
Co-Ru/MWCNTs	14.9	(Trépanier et al., 2009)
Co/CNTs	15.4	(Davari et al., 2014)
Co/rGO	19.5	(Jiang et al., 2021)
Co/GNS	21.6	(Karimi et al., 2015a)
Co/NGA	23.2	(Wang et al., 2020)

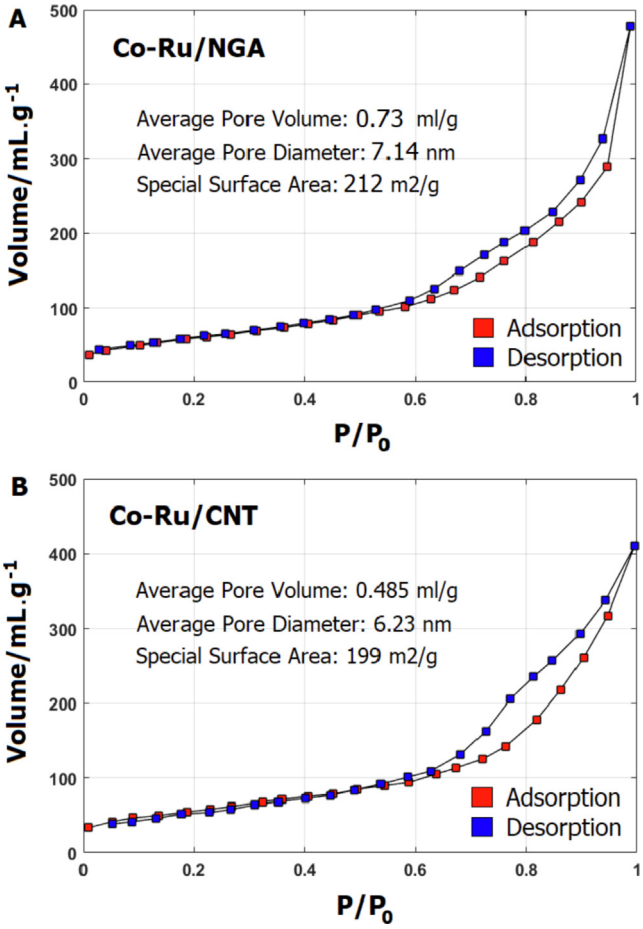

Fig. 3 Depicts the N_2 physisorption isotherms of Co-Ru/NGA (a) and Co-Ru/CNT (b); calcined at 400 °C for 4 h.

Table 1 The ICP results of the prepared catalysts.

Catalyst	Cobalt loading (%)		Ru loading (%)	
	Theory	ICP	Theory	ICP
Co-Ru/NGA	50	49.52	1	0.84
Co-Ru/CNT	50	48.75	1	0.92

trend for both catalysts. The average pore volume of Co-Ru/NGA and Co-Ru/CNT were 0.73 and 0.48 mL g^{-1}, respectively.

Recent studies have evaluated the BET surface area and pore structure of catalysts for the Fischer-Tropsch process (Fang et al., 2021; Li et al., 2022). For example, cobalt-based catalysts supported on mesoporous silica (Co/SiO_2) synthesized exhibited a BET surface area of 257 $m^2 g^{-1}$ and a pore volume of 0.8 ml g^{-1} while iron-based catalysts supported on mesoporous silica (Fe/SiO_2) synthesized exhibited BET surface areas in the range of 215–250 $m^2 g^{-1}$ with average pore volumes ranging from 0.56 to 0.67 ml g^{-1}. Additionally, cobalt-based catalysts supported on carbon nanotubes (Co/CNT) synthesized exhibited a BET surface area of 298 $m^2 g^{-1}$ and a pore volume of 0.7 ml g^{-1}. These studies showed that catalysts with BET surface areas in the range of 200–300 $m^2 g^{-1}$ and pore volumes of 0.5–0.8 ml g^{-1} can exhibit high catalytic activity and selectivity for the Fischer-Tropsch process, highlighting the importance of carefully tuning the BET surface area and pore structure of catalysts for optimal performance.

The comparable BET indicates that both catalysts can be used in the Fischer-Tropsch process. The studies on cobalt-based and iron-based catalysts supported on mesoporous silica and cobalt-based catalysts supported on carbon nanotubes further highlight the importance of tuning the BET surface area and pore structure for optimal catalytic activity and selectivity in the Fischer-Tropsch process.

3.4. XRD results

The detection of crystalline phases of Co-Ru catalysts on nitrogen-doped graphene aerogel (Fig. 4**a**) and carbon nanotubes (Fig. 4**b**) was achieved using X-ray diffraction (XRD) analysis. The peaks observed at 2θ = 25° and 2θ = 43° were attributed to the nitrogen-doped graphene aerogel, while the peaks detected at 2θ = 32°, 37°, 55°, 60°, and 65° corresponded to cobalt oxide that had formed on the surface of the graphene. The sharpest peak was observed at an angle of 2θ = 37°. Previous research (Sasson Bitters et al., 2022) suggests that the cobalt oxide detected in the XRD pattern is most likely Co_3O_4. In the XRD patterns, a distinct peak of ruthenium oxide is observed at 2θ = 30°. The size of cobalt particles in Co-Ru catalysts supported on nitrogen-doped graphene aerogel (NGA) and carbon nanotubes (CNT) was evaluated using Scherer's equation. Table 4 shows that the larger surface area of graphene in NGA leads to better particle dispersion and a smaller crystallite size of cobalt oxide compared to CNT. Additionally, the size of cobalt oxide nanocrystals in bimetallic catalysts with ruthenium was found to be larger than in monometallic catalysts due to the reduction in the number of cobalt oxide crystal sites and the formation of a bimetallic catalyst.

3.5. EDX

Energy Dispersive X-ray Spectroscopy (EDX) is a powerful analytical technique used to determine the elemental composition of a sample. In the case of Co-Ru/CNT and Co-Ru/NGA catalysts, EDX can provide information on the elemental

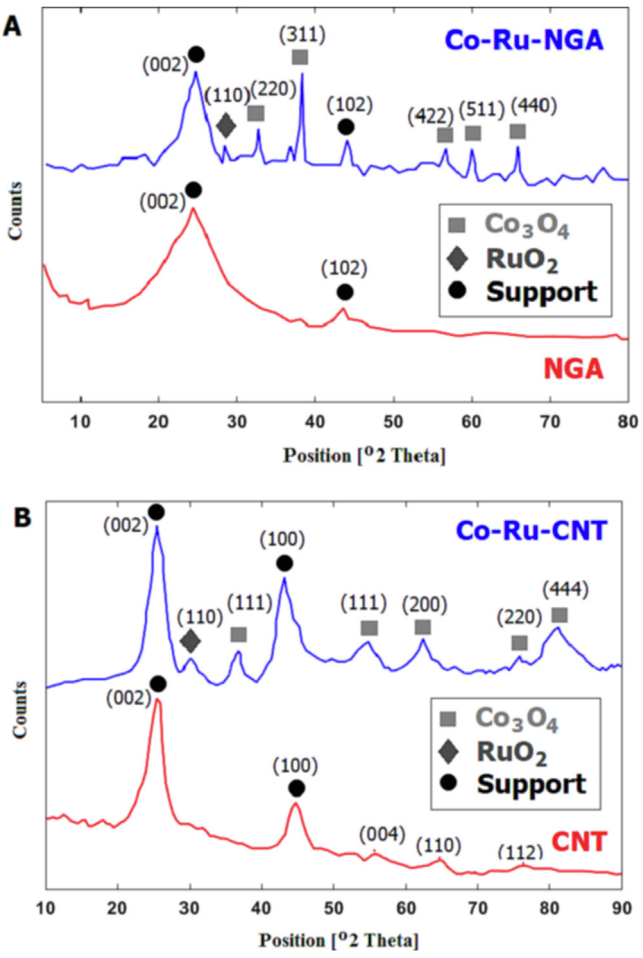

Fig. 4 XRD patterns of NGA, Co-Ru/NGA (a) and CNT, Co-Ru/CNT (b) catalysts.

composition of the Co-Ru/CNT and Co-Ru/NGA themselves, as well as any coatings or functionalizations on their surfaces. In this study, cobalt peaks were observed in Co-Ru/CNT and Co-Ru/NGA catalysts at 0.8 and 7 keV, and ruthenium peaks in form of Ru L α and Ru L β appeared at 2.4 and 2.6 KeV, respectively (Fig. 5).

In a study by Shariati et al. (Shariati et al., 2019), carbon nanotubes were coated with cobalt and ruthenium using a chemical vapor deposition method. The authors used EDX to confirm the presence of both cobalt and ruthenium on the CNT surfaces. The EDX spectra showed peaks corresponding to cobalt and ruthenium at energy levels of approximately 0.8 keV and 2.2 keV, respectively. These energy levels are characteristic of the Kα X-rays of cobalt and ruthenium, which are emitted when electrons transition from the L-shell to the K-shell of the respective elements. In another study by Mosayebi et al. (Mosayebi et al., 2016), carbon nanotubes were coated with a thin layer of cobalt using a chemical reduction method. The authors used EDX to confirm the presence of cobalt on the CNT surfaces and found peaks corresponding to cobalt at an energy level of approximately 0.8 keV, consistent with the Kα X-ray of cobalt.

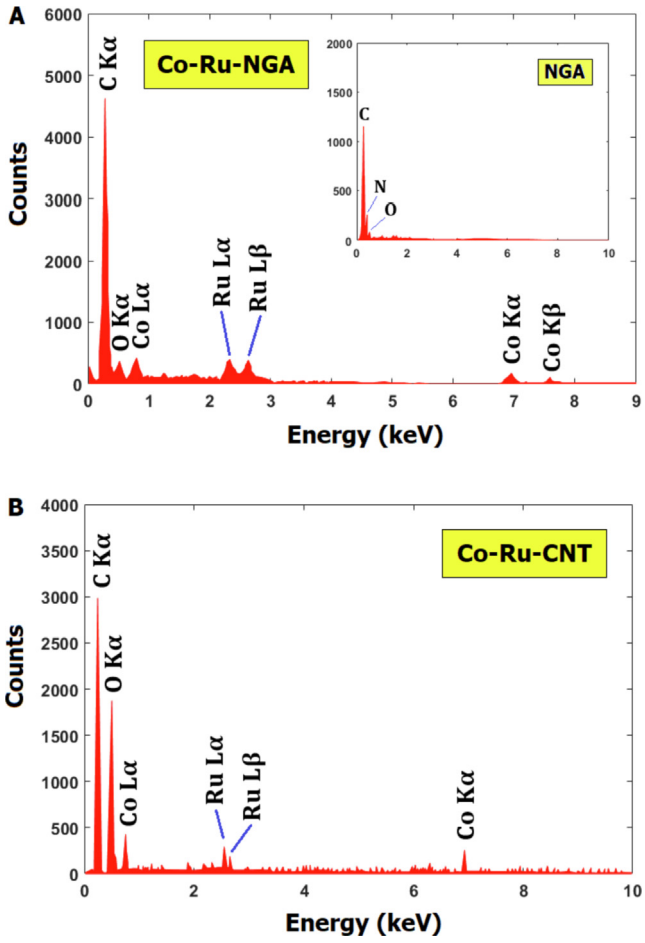

Fig. 5 EDX analysis of Co-Ru/NGA (a) and Co-Ru/CNT (b) catalysts.

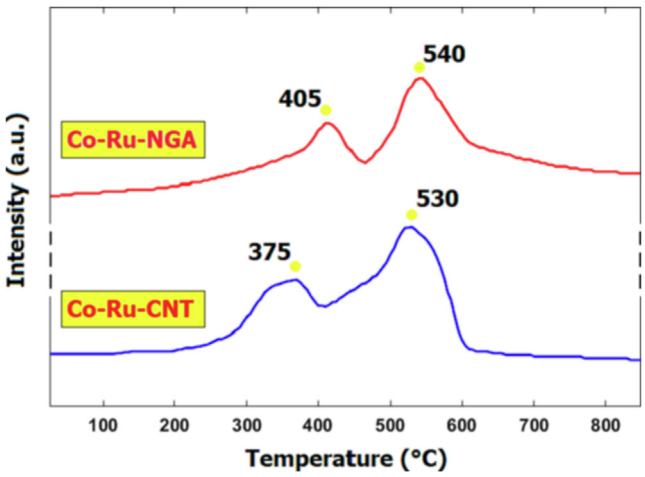

Fig. 6 TPR patterns of the Co-Ru/NGA and Co-Ru/CNT catalysts.

3.6. TPR results

The H_2-TPR profiles of the catalysts were measured to study the reducibility of the Co and Ru species supported on CNT and NGA. As shown in the H_2-TPR profiles in Fig. 6, Co-Ru/CNT exhibits a relatively lower reduction temperature compared with Co-Ru/NGA, indicating that the former has higher reducibility than the latter. This suggests that the Co-Ru/CNT catalyst may have a larger number of low-valence Co and Ru species than Co-Ru/NGA. In addition to the type of support material, the metal concentration also plays a crucial role in determining the reducibility of the catalysts. Several studies have investigated the effect of metal loading on the TPR profiles of Co-Ru catalysts supported on nitrogen-doped graphene aerogel or carbon nanotubes (Table 3). For instance, Bepari et al. (Bepari et al., 2020) reported that the reduction temperature of Co-Ru/Graphene oxide catalysts decreased with an increase in the metal loading, which was attributed to the formation of smaller Co and Ru particles at higher metal loadings. Similarly, Karimi et al. (Karimi et al., 2019) found that the reduction peaks of Co-Ru/CNT catalysts shifted towards lower temperatures with increasing metal loading. They suggested that the high metal loading resulted in the formation of a large number of small Co and Ru particles, which were more easily reduced than the larger particles. Overall, these studies indicate that the metal loading has a significant effect on the reducibility of the Co-Ru catalysts supported on graphene or carbon nanotubes. The type of metal in a catalyst can have a significant effect on its TPR behavior. For example, a study by Abbas et al. (Abbas et al., 2020) found that the reducibility of Co-based catalysts was generally higher than that of Ni-based catalysts, which was attributed to the stronger metal-support interaction in Co-based catalysts. Additionally, the size and dispersion of the metal particles can also affect the TPR behavior. For instance, a study by Mierczyński (Mierczyński et al., 2022) found that increasing the loading of Pt on carbon nanotubes led to a decrease in the reduction temperature, indicating that smaller Pt particles had higher reducibility. Overall, the type of metal and its dispersion on the support can strongly influence the TPR behavior of a catalyst.

3.7. TPD results

In this work, two catalysts, Co-Ru/CNT and Co-Ru/NGA, were analyzed using temperature programmed desorption (TPD) to investigate their hydrogen (H_2) uptake and desorption properties (Table 4). TPD is a commonly used technique for studying the adsorption and desorption of gases on catalyst surfaces.

The H_2 uptake and desorption properties of the two catalysts were compared, and the results showed that the Co-Ru/CNT catalyst had a higher H_2 uptake value of 0.982 mmol g^{-1}, compared to Co-Ru/NGA with a value of 0.853 mmol g^{-1} both catalysts had a desorption temperature of 400 °C.

The dispersion and reduction properties of the catalysts were also investigated, and the Co-Ru/CNT catalyst had a higher dispersion percentage of 87%, compared to 92% for Co-Ru/NGA. The reduction percentage of Co-Ru/CNT was 4% compared to 3.2% for Co-Ru/NGA. The particle size of Co-Ru/CNT was found to be 4 nm, slightly larger than the 3.2 nm particle size of Co-Ru/NGA.

The TPD analysis results suggest that the Co-Ru/CNT catalyst has a higher H_2 uptake, dispersion, and reduction per-

Table 3 TPR analysis for Co-Ru/NGA and Co-Ru/CNT catalysts and comparison with results from other studies.

Catalyst	Main Reduction Peaks	Additional Information	Reference
Co-Ru/NGA	405 °C (CoO), 540 °C (RuO)	The hydrogen consumption peak for carbon species is observed in the 400–600 °C temperature range.	In this study
Co-Ru/CNT	375 °C (CoO), 530 °C (RuO)	In the Co-Ru/CNT catalyst, the hydrogen consumption peak for carbon species on the carbonaceous support of CNT is observed at around 500–550 °C in the H_2-TPR profile.	In this study
Ru/Graphite	480 °C (RuO)	Interaction between metal species and graphene support affected reducibility.	(Gonzalo-Chacón et al., 2014)
Co/GNS	350 °C (CoO)	H2-TPR provided insight into interaction between Co species and graphene support.	(Karimi et al., 2015a)
Ru/N-GNS	225 °C, 525 °C (RuO)	H2-TPR provided information on reducibility of metal species and effect of graphene support on electronic properties.	(Taghavi et al., 2019)
Co/GNS	400 °C (CoO)	Stronger interaction between Co species and graphene support attributed to shift of reduction peak to lower temperature.	(Taghavi et al., 2017)
Ru/GNS	380–560 °C (RuO)	Broad reduction peak attributed to presence of multiple RuOx species with different reducibilities due to interaction between Ru species and graphene support.	(Hemmati et al., 2012)
Co-Ru/CNT	300 °C (CoO), 450 °C (RuO)	Cobalt and ruthenium species had strong interaction with CNT support, enhancing their reducibility.	(Shariati et al., 2019)
Co/CNT	200 °C (CoO)	Cobalt species had weak interaction with CNT support.	(Karimi et al., 2015b)
Ru/CNT	320 °C (RuO)	Ruthenium species had weak interaction with CNT support.	(Bahome et al., 2007)

Table 4 H_2-TPD data of catalysts.

Catalyst	H_2uptake (mmolg^{-1})	H_2desorption (°C)	Dispersion (%)	Reduction (%)	$d_{particles}$(nm)	Reference
Co-Ru/NGA	0.853	400	51	92	3.2	In this work
Co-Ru/CNT	0.982	400	42	87	4	In this work
Co-Ru/CNT	0.79	400	50	78	3.6	(Tavasoli and Taghavi, 2013)
Co/CNT	1.08	395	43	84	3.8	(Eschemann et al., 2015)
Co/GNS	0.62	355	58	91	2.9	(Karimi et al., 2015a)
Ru/GNS	0.58	370	52	89	3.1	(Guo et al., 2022)

centage than the Co-Ru/NGA catalyst. However, Co-Ru/NGA has a smaller particle size, which could potentially lead to higher catalytic activity. These findings demonstrate the importance of carefully considering the properties of catalysts when selecting them for specific applications.

3.8. TEM

The results of the TEM analysis for the catalysts are presented in Fig. 7**.** The images clearly depict the spherical shape of cobalt oxide nanoparticles on the surface of nitrogen-doped graphene aerogel and carbon nanotubes, which appear as dark spots. It is evident from the TEM images that the cobalt nanoparticles are evenly distributed on the support surface, with a particle size ranging between 10 and 20 nm. The average particle size of the cobalt oxide nanoparticles is approximately 13–12 nm, which is in agreement with the findings from the XRD analysis.

3.9. Catalyst results

The Fischer-Tropsch process is a catalytic process that converts syngas, a mixture of carbon monoxide (CO) and hydrogen (H_2), into higher-value hydrocarbons. Co-Ru/NGA and Co-Ru/CNT catalysts are two promising catalysts for the Fischer-Tropsch process, as shown in the table above. The reactor used for the Fischer-Tropsch process typically consists of a fixed-bed reactor packed with the catalyst material. The syngas is fed into the reactor at a certain flow rate and pressure, and the reaction takes place in the presence of the catalyst. The FT process is highly exothermic, and the reactor must be carefully designed to control the temperature to prevent catalyst deactivation due to overheating.

In the Fischer-Tropsch test, a catalyst mass of 0.5 g was loaded into the reactor. The reactor temperature was set at 260 °C for Co-Ru/CNT and 280 °C for Co-Ru/NGA. The presence of feed was ensured by introducing syngas, which is

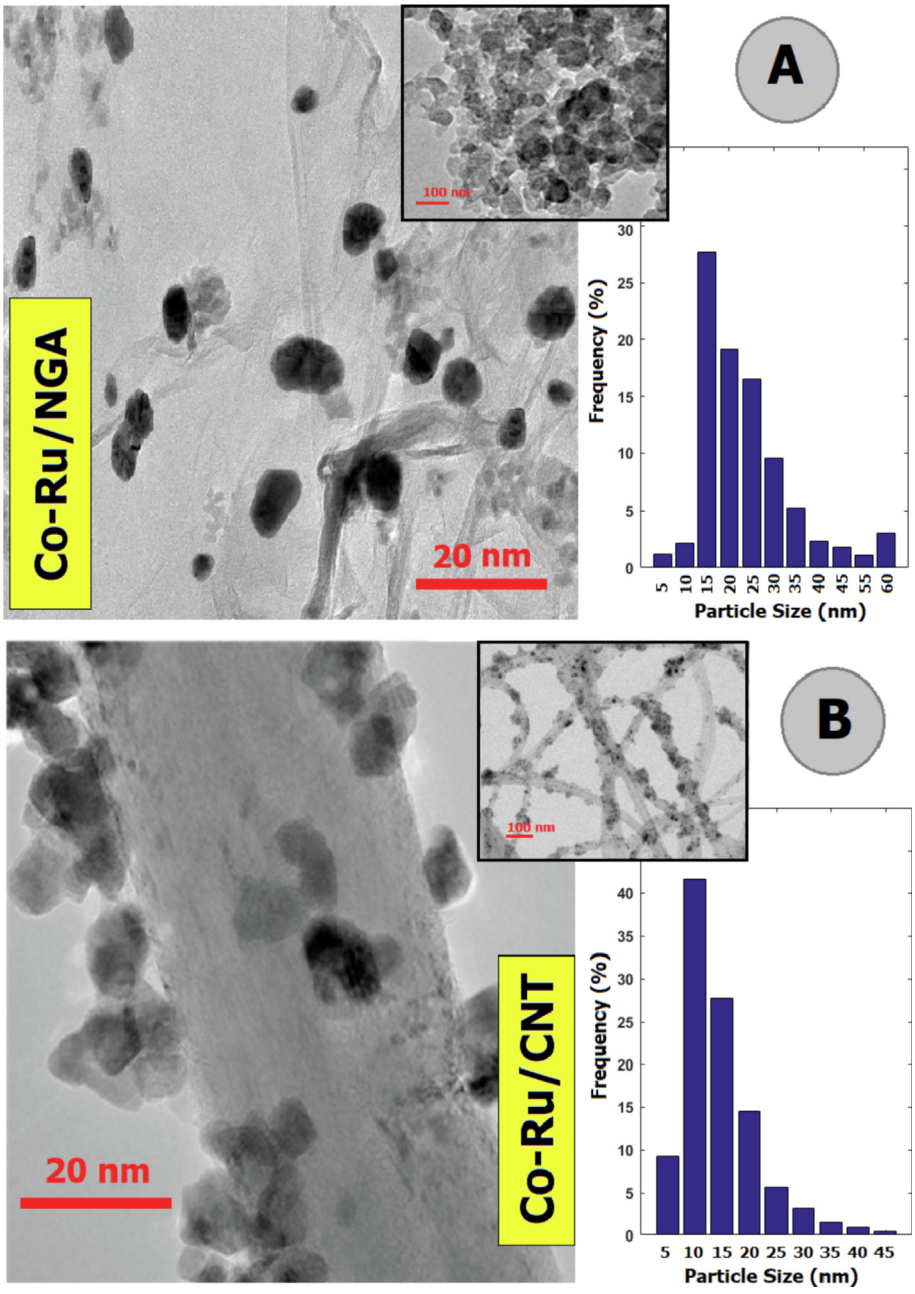

Fig. 7 TEM images of Co-Ru/NGA and Co-Ru/CNT catalysts.

a mixture of hydrogen (H_2) and carbon monoxide (CO). The H_2 : CO ratio was 2:1 for Co-Ru/CNT and 1:1 for Co-Ru/NGA, and the pressure was maintained at 25 bar. The Gas Hourly Space Velocity (GHSV) was set to 10,000 ml g^{-1} h^{-1}. According to Table 5, the results showed that both catalysts had optimal temperature ranges, pressure ranges, and H_2 : CO feed ratios for the production of hydrocarbons. The Co-Ru/CNT catalyst had a higher selectivity for C_5^+ hydrocarbons, while the Co-Ru/NGA catalyst had a higher selectivity for methane. Both catalysts demonstrated good stability over a 50-hour test period, with no significant loss of activity or selectivity.

In Table 5, the results of this study were compared with the results of other studies. It was observed that the addition of a second metal to the catalyst can have a significant impact on its performance. For example, the Co-Ru/CNT catalyst was found to have higher selectivity towards C_5^+ hydrocarbons compared to Co/CNT catalyst, which indicates the positive effect of adding a second metal. In this study, the bimetallic Co-Ru catalyst showed improved selectivity towards C_5^+ hydrocarbons compared to the monometallic Co catalyst, which also supports the finding that bimetallic catalysts can have enhanced performance. Overall, the results obtained in this study were consistent with the findings of previous

Table 5 Catalytic performance of Co-Ru/NGA and Co-Ru/CNT catalysts in of Fischer-Tropsch synthesis.

Catalyst	Pressure (bar)	Temperature (°C)	GHSV ($mlg^{-1}h^{-1}$)	H_2 : CO	CO Conversion (%)	FTS rate ($g_{CH}g_{Cat}^{-1}h^{-1}$)	Selectivity (%)				Reference
							CO_2	CH_4	C2–C4	C_{5+}	
Co-Ru/NGA	25	280	10,000	1:1	75.25	0.382	0.5	70.5	11.3	17.2	In this work
Co-Ru/CNT	25	260	10,000	2:1	73.42	0.325	0.7	23.5	12	63.7	In this work
Ru/CNT	1.5	240	1800	2	98.2	0.84	1.8	64.6	31.0	4.4	(Xiong et al., 2010)
Co/GNS	1	220	3600	2	95.2	0.43	8.8	0.1	16.7	83.2	(Okoye-Chine et al., 2019)
Co/CNT	1	220	6000	2:1	95.1	1.86	2.6	81.5	13.6	2.3	(Lu et al., 2023)
Co/CNT	1	220	1400	2:1	96.3	1.78	2.5	80.5	14.5	2.5	(Shariati et al., 2019)
Co-Ru/CNT	3	220	1400	2:1	95.0	2.44	2.8	77.0	16.5	4.5	(Shariati et al., 2019)

research, highlighting the importance of the type of catalyst used and the effect of adding a second metal to the catalyst for improving selectivity towards C_5^+ hydrocarbons in the Fischer-Tropsch process.

4. Conclusions

In this study, we investigated the performance of two catalysts, Co-Ru/CNT and Co-Ru/NGA, in the Fischer-Tropsch process. The catalysts were characterized using various techniques, including XRD, TPD, and TEM, to evaluate their properties and performance. The results showed that both catalysts had optimal temperature ranges, pressure ranges, and H_2 : CO feed ratios for the production of hydrocarbons, and demonstrated good stability over a 50-hour test period, with no significant loss of activity or selectivity. However, the Co-Ru/CNT catalyst had a higher H_2 uptake, dispersion, and reduction percentage than the Co-Ru/NGA catalyst, which could potentially lead to higher catalytic activity. Additionally, the Co-Ru/CNT catalyst had a higher selectivity for C_{5+} hydrocarbons, while the Co-Ru/NGA catalyst had a higher selectivity for methane. These findings suggest that the choice of catalyst is crucial for the production of desired hydrocarbons in the Fischer-Tropsch process. Furthermore, the results indicated that the addition of a second metal to the catalyst can have a significant impact on its performance, as observed with the Co-Ru/CNT catalyst. Bimetallic catalysts were found to have improved selectivity towards C_{5+} hydrocarbons compared to monometallic catalysts, highlighting the importance of the type of catalyst used and the effect of adding a second metal to the catalyst for improving selectivity towards desired hydrocarbons in the Fischer-Tropsch process. Overall, this study provides valuable insights into the properties and performance of Co-Ru/CNT and Co-Ru/NGA catalysts in the Fischer-Tropsch process, and highlights the need for careful selection of catalysts for specific applications. These findings can be useful for the development of more efficient and effective catalysts for the production of desired hydrocarbons in the Fischer-Tropsch process.

Declaration of Competing Interest

The authors declare that they have no known competing financial interests or personal relationships that could have appeared to influence the work reported in this paper.

References

Abbas, M., Zhang, J., Mansour, T.S., Chen, J., 2020. Hierarchical porous spinel MFe_2O_4 (M = Fe, Zn, Ni and Co) nanoparticles: Facile synthesis approach and their superb stability and catalytic performance in Fischer-Tropsch synthesis. Int. J. Hydrogen Energy 45, 10754–10763. https://doi.org/10.1016/j.ijhydene.2020.02.044.

Bahome, M.C., Jewell, L.L., Padayachy, K., Hildebrandt, D., Glasser, D., Datye, A.K., Coville, N.J., 2007. Fe-Ru small particle bimetallic catalysts supported on carbon nanotubes for use in Fischer-Tröpsch synthesis. Appl. Catal. A 328, 243–251. https://doi.org/10.1016/j.apcata.2007.06.018.

Bepari, S., Li, X., Abrokwah, R., Mohammad, N., Arslan, M., Kuila, D., 2020. Co-Ru catalysts with different composite oxide supports for Fischer-Tropsch studies in 3D-printed stainless steel microreactors. Appl. Catal. A 608,. https://doi.org/10.1016/j.apcata.2020.117838 117838.

Cheng, Q., Liu, Y., Lyu, S., Tian, Y., Ma, Q., Li, X., 2021. Manipulating metal-support interactions of metal catalysts for Fischer-Tropsch synthesis. Chinese J. Chem. Eng. 35, 220–230. https://doi.org/10.1016/j.cjche.2021.05.013.

Davari, M., Karimi, S., Tavasoli, A., Karimi, A., 2014. Enhancement of activity, selectivity and stability of CNTs-supported cobalt catalyst in Fischer-Tropsch via CNTs functionalization. Appl. Catal. A 485, 133–142. https://doi.org/10.1016/j.apcata.2014.07.023.

Detsios, N., Zisopoulos, G., Atsonios, K., Nikolopoulos, N., Grammelis, P., Kaltenmorgen, J., 2022. Dynamic process simulations and control of a lignite/waste to Fischer Tropsch liquids plant. Fuel Process. Technol. 236. https://doi.org/10.1016/j.fuproc.2022.107395.

dos Santos, R.G., Alencar, A.C., 2020. Biomass-derived syngas production via gasification process and its catalytic conversion into fuels by Fischer Tropsch synthesis: a review. Int. J. Hydrogen Energy 45, 18114–18132. https://doi.org/10.1016/j.ijhydene.2019.07.133.

Eschemann, T.O., Lamme, W.S., Manchester, R.L., Parmentier, T.E., Cognigni, A., Rønning, M., De Jong, K.P., 2015. Effect of support surface treatment on the synthesis, structure, and performance of Co/CNT Fischer-Tropsch catalysts. J. Catal. 328, 130–138. https://doi.org/10.1016/j.jcat.2014.12.010.

Fang, G., Lin, J., Wang, X., 2021. Low-temperature conversion of methane to oxygenates by supported metal catalysts: from nanoparticles to single atoms. Chinese J. Chem. Eng. 38, 18–29. https://doi.org/10.1016/j.cjche.2021.04.034.

Gonzalo-Chacón, L., Almohalla, M., Gallegos-Suarez, E., Guerrero-Ruiz, A., Rodríguez-Ramos, I., 2014. Effects of the reduction temperature over ex-chloride Ru Fischer-Tropsch catalysts supported on high surface area graphite and promoted by potassium. Appl. Catal. A 480, 86–92. https://doi.org/10.1016/j.apcata.2014.04.046.

Guo, L., Guo, Z., Liang, J., Yong, X., Sun, S., Zhang, W., Sun, J., Zhao, T., Li, J., Cui, Y., Zhang, B., Yang, G., Tsubaki, N., 2022. Quick microwave assembling nitrogen-regulated graphene supported iron nanoparticles for Fischer-Tropsch synthesis. Chem. Eng. J. 429,. https://doi.org/10.1016/j.cej.2021.132063 132063.

Hemmati, M.R., Kazemeini, M., Khorasheh, F., Zarkesh, J., Rashidi, A., 2012. Cobalt supported on CNTs-covered γ- And nanostructured alumina catalysts utilized for wax selective Fischer-Tropsch synthesis. J. Nat. Gas Chem. 21, 713–721. https://doi.org/10.1016/S1003-9953(11)60424-6.

Hodala, J.L., Moon, D.J., Reddy, K.R., Reddy, C.V., Kumar, T.N., Ahamed, M.I., Raghu, A.V., 2021. Catalyst design for maximizing C_{5+} yields during Fischer-Tropsch synthesis. Int. J. Hydrogen Energy 46, 3289–3301. https://doi.org/10.1016/j.ijhydene.2019.12.021.

Jiang, J., Duan, D., Ma, J., Jiang, Y., Long, R., Gao, C., Xiong, Y., 2021. Van der waals heterostructures by single cobalt sites-anchored graphene and g-C_3N_4 nanosheets for photocatalytic syngas production with tunable CO/H_2 ratio. Appl. Catal. B Environ. 295,. https://doi.org/10.1016/j.apcatb.2021.120261 120261.

Julkapli, N.M., Bagheri, S., 2015. Graphene supported heterogeneous catalysts: an overview. Int. J. Hydrogen Energy 40, 948–979. https://doi.org/10.1016/j.ijhydene.2014.10.129.

Karimi, S., Tavasoli, A., Mortazavi, Y., Karimi, A., 2015a. Enhancement of cobalt catalyst stability in Fischer-Tropsch synthesis using graphene nanosheets as catalyst support. Chem. Eng. Res. Des. 104, 713–722. https://doi.org/10.1016/j.cherd.2015.10.016.

Karimi, S., Tavasoli, A., Mortazavi, Y., Karimi, A., 2015b. Cobalt supported on Graphene - A promising novel Fischer-Tropsch synthesis catalyst. Appl. Catal. A 499, 188–196. https://doi.org/10.1016/j.apcata.2015.04.024.

Karimi, S., Tavakkoli Yaraki, M., Karri, R.R., 2019. A comprehensive review of the adsorption mechanisms and factors influencing the adsorption process from the perspective of bioethanol dehydration. Renew. Sustain. Energy Rev. 107, 535–553. https://doi.org/10.1016/j.rser.2019.03.025.

Li, Z., Li, M., Bian, Z., Kathiraser, Y., Kawi, S., 2016. Design of highly stable and selective core/yolk-shell nanocatalysts-review. Appl. Catal. B Environ. 188, 324–341. https://doi.org/10.1016/j.apcatb.2016.01.067.

Li, M., Li, Z., Lin, Q., Cao, J., Liu, F., Kawi, S., 2022. Synthesis strategies of carbon nanotube supported and confined catalysts for thermal catalysis. Chem. Eng. J. 431,. https://doi.org/10.1016/j.cej.2021.133970 133970.

Liu, Y., Lu, F., Tang, Y., Liu, M., Tao, F.F., Zhang, Y., 2020. Effects of initial crystal structure of Fe_2O_3 and Mn promoter on effective active phase for syngas to light olefins. Appl. Catal. B Environ. 261. https://doi.org/10.1016/j.apcatb.2019.118219.

Lu, W., Wang, J., Ma, Z., Chen, C., Liu, Y., Hou, B., Li, D., Wang, B., 2023. Classifying and understanding the role of carbon deposits on cobalt catalyst for Fischer-Tropsch synthesis. Fuel 332,. https://doi.org/10.1016/j.fuel.2022.126115 126115.

Mierczyński, P., Dawid, B., Mierczynska-Vasilev, A., Maniukiewicz, W., Witońska, I., Vasilev, K., Szynkowska-Jóźwik, M.I., 2022. Novel bimetallic 1%M-Fe/Al_2O_3-Cr_2O_3 (2:1) (M = Ru, Au, Pt, Pd) catalysts for Fischer-Tropsch synthesis. Catal. Commun. 172. https://doi.org/10.1016/j.catcom.2022.106559.

Mosayebi, A., Mehrpouya, M.A., Abedini, R., 2016. The development of new comprehensive kinetic modeling for Fischer-Tropsch synthesis process over Co-Ru/γ-Al_2O_3 nano-catalyst in a fixed-bed reactor. Chem. Eng. J. 286, 416–426. https://doi.org/10.1016/j.cej.2015.10.087.

Okoye-Chine, C.G., Moyo, M., Liu, X., Hildebrandt, D., 2019. A critical review of the impact of water on cobalt-based catalysts in Fischer-Tropsch synthesis. Fuel Process. Technol. 192, 105–129. https://doi.org/10.1016/j.fuproc.2019.04.006.

Piazzi, S., Patuzzi, F., Baratieri, M., 2022. Energy and exergy analysis of different biomass gasification coupled to Fischer-Tropsch synthesis configurations. Energy 249,. https://doi.org/10.1016/j.energy.2022.123642 123642.

Sapountzi, F.M., Gracia, J.M., Weststrate, C.J., Kee, J., Fredriksson, H.O.A., Niemantsverdriet, J.W., Hans, 2017. Electrocatalysts for the generation of hydrogen, oxygen and synthesis gas. Prog. Energy Combust. Sci. 58, 1–35. https://doi.org/10.1016/j.pecs.2016.09.001.

Sasson Bitters, J., He, T., Nestler, E., Senanayake, S.D., Chen, J.G., Zhang, C., 2022. Utilizing bimetallic catalysts to mitigate coke formation in dry reforming of methane. J. Energy Chem. 68, 124–142. https://doi.org/10.1016/j.jechem.2021.11.041.

Shariati, J., Haghtalab, A., Mosayebi, A., 2019. Fischer-Tropsch synthesis using Co and Co-Ru bifunctional nanocatalyst supported on carbon nanotube prepared via chemical reduction method. J. Energy Chem. 28, 9–22. https://doi.org/10.1016/j.jechem.2017.10.001.

Taghavi, S., Asghari, A., Tavasoli, A., 2017. Enhancement of performance and stability of Graphene nano sheets supported cobalt catalyst in Fischer-Tropsch synthesis using Graphene functionalization. Chem. Eng. Res. Des. 119, 198–208. https://doi.org/10.1016/j.cherd.2017.01.021.

Taghavi, S., Tavasoli, A., Asghari, A., Signoretto, M., 2019. Loading and promoter effects on the performance of nitrogen functionalized graphene nanosheets supported cobalt Fischer-Tropsch synthesis catalysts. Int. J. Hydrogen Energy 44, 10604–10615. https://doi.org/10.1016/j.ijhydene.2019.03.015.

Tavasoli, A., Taghavi, S., 2013. Performance enhancement of bimetallic Co-Ru/CNTs nano catalysts using microemulsion technique. J. Energy Chem. 22, 747–754. https://doi.org/10.1016/S2095-4956(13)60099-6.

Trépanier, M., Tavasoli, A., Dalai, A.K., Abatzoglou, N., 2009. Co, Ru and K loadings effects on the activity and selectivity of carbon nanotubes supported cobalt catalyst in Fischer-Tropsch synthesis. Appl. Catal. A 353, 193–202. https://doi.org/10.1016/j.apcata.2008.10.061.

Vasseghian, Y., Le, V.T., Joo, S.W., Dragoi, E.N., Kamyab, H., Chelliapan, S., Klemeš, J.J., 2022. Spotlighting graphene-based catalysts for the mitigation of environmentally hazardous pollutants to cleaner production: A review. J. Clean. Prod. 365. https://doi.org/10.1016/j.jclepro.2022.132702.

Wang, C., Astruc, D., 2018. Recent developments of metallic nanoparticle-graphene nanocatalysts. Prog. Mater Sci. 94, 306–383. https://doi.org/10.1016/j.pmatsci.2018.01.003.

Wang, B., Han, Y., Chen, S., Zhang, Y., Li, J., Hong, J., 2020. Construction of three-dimensional nitrogen-doped graphene aerogel (NGA) supported cobalt catalysts for Fischer-Tropsch synthesis. Catal. Today 355, 10–16. https://doi.org/10.1016/j.cattod.2019.03.009.

Xiong, K., Li, J., Liew, K., Zhan, X., 2010. Preparation and characterization of stable Ru nanoparticles embedded on the ordered mesoporous carbon material for applications in Fischer-Tropsch synthesis. Appl. Catal. A 389, 173–178. https://doi.org/10.1016/j.apcata.2010.09.012.